Dynamic evolution of the spectrum of long-period fiber Bragg gratings fabricated from hydrogen-loaded optical fiber by ultraviolet laser irradiation

Keio Fujita, Yuji Masuda, Keisuke Nakayama, Maki Ando, Kenji Sakamoto,
Jun-pei Mohri, Makoto Yamauchi, Masanori Kimura, Yasuo Mizutani,
Susumu Kimura, Takashi Yokouchi, Yoshifumi Suzaki, and Seiki Ejima

Long-period fiber Bragg gratings fabricated by exposure of hydrogen-loaded fiber to UV laser light exhibit large-scale dynamic evolution for approximately two weeks at room temperature. During this time two distinct features show up in their spectrum: a large upswing in wavelength and a substantial deepening of the transmission minimum. The dynamic evolution of the transmission spectrum is explained quantitatively by use of Malo's theory of UV-induced quenching [Electron. Lett. **30,** 442 (1994)] followed by refilling of hydrogen in the fiber core and the theory of hydrogen diffusion in the fiber material. The amount of hydrogen quenched by the UV irradiation is 6% of the loaded hydrogen.   © 2005 Optical Society of America

OCIS codes: 050.2770, 060.2310, 060.2340, 160.5340.

1. Introduction

Long-period fiber Bragg gratings (LP-FBGs), which have a periodic structure in the refractive index in the longitudinal direction of the fiber with a period of ~ 0.5 mm, convert incident light in the fundamental LP_{01} mode into higher-order LP_{0m} modes through mode coupling. Because the higher-order modes cannot propagate in a single-mode fiber but are lost outside the fiber, a LP-FBG works as an attenuator. Owing to the wavelength dependence of the attenuation, LP-FBGs are utilized extensively for applications such as equalizing light sources and optical amplifiers to flatten the wavelength dependence of their outputs.

LP-FBGs are commonly produced by exposure of an optical fiber to UV laser light in a manner similar to that used for fabricating short-period fiber Bragg gratings (SP-FBGs). Their optical spectrum is known to exhibit large scale dynamic evolution after fabrication. At room temperature, their wavelength increases by several tens to hundreds of nanometers and decrease thereafter. Also, the transmission minimum becomes deeper over that time as if the strength of the grating modulation were increasing.

Bakhti *et al.* have shown that the large upswing in the LP-FBG wavelength is due to diffusion of the hydrogen loaded into the fiber before exposure to UV laser light to enhance the fiber's UV photosensitivity.[1] The wavelength of the LP-FBG is given by

$$\lambda = \left(n_{\mathrm{eff}}{}^{01} - n_{\mathrm{eff}}{}^{0m} \right)\Lambda, \qquad (1)$$

where $n_{\mathrm{eff}}{}^{01}$ and $n_{\mathrm{eff}}{}^{0m}$ are the effective refractive indices for the LP_{01} and LP_{0m} modes and Λ is the grating period. Because the intensity of fundamental mode LP_{01} is concentrated in the fiber core, $n_{\mathrm{eff}}{}^{01}$ should be close to the index of the core, n_{core}. Similarly, as the intensity of higher mode LP_{0m} is distributed over the fiber's cross section, $n_{\mathrm{eff}}{}^{0m}$ reflects the

index of the fiber cladding, n_{clad} because the cross-sectional area is dominated by the cladding.

The hydrogen loaded into the fiber starts to diffuse out from the fiber when it is exposed to the laser light. During this outdiffusion the hydrogen concentration decreases initially in the outer portion of the fiber cladding and later in the central fiber core. Consequently, as the hydrogen concentration evolves, the component of the refractive index that is due to the presence of hydrogen causes first n_{eff}^{0m} and then n_{eff}^{01} to decrease. In Eq. (1), the second term decreases early in time and the first term decreases later on; this means that the wavelength undergoes an upswing. Bakhti *et al.* have demonstrated that the wavelength evolves in this way by comparison with theoretical calculations.[1] The behavior of the transmission minimum of the spectrum has not, however, been explained.

An upswing of the wavelength is also seen in SP-FBGs but for a different physical reason. The wavelength of a SP-FBG fabricated by exposure of hydrogen-loaded fiber to UV laser light exhibits an increase within ~5 h and a decrease by 0.7–1 nm to the initial value after ~200 h at room temperature. Malo *et al.* explained this upswing in the wavelength in terms of quenching of hydrogen at the fiber core.[2] The UV irradiation induces photodissociation of molecular hydrogen. Some of the dissociated atoms react in the fiber core to form a Ge–OH bond followed by creation of oxygen deficiencies, while the rest of the atoms recombine into molecules. The consumption of hydrogen in Ge–OH formation has the effect of quenching hydrogen molecules in the fiber core. In the cladding region the hydrogen concentration does not change because the dissociated atoms simply recombine there without reacting otherwise. Then the hydrogen in the cladding surrounding the core starts to diffuse inward to refill the depleted core region. Thus the wavelength of the SP-FBG, which is given by

$$\lambda = 2n_{eff}^{01}\Lambda, \qquad (2)$$

increases through effective refractive index n_{eff}^{01} by an amount that corresponds to the replacement of the hydrogen in the depleted core. Later the wavelength decreases as all the hydrogen diffuses out of the fiber.

We have found experimentally and theoretically that the evolution of both the wavelength and the transmission minimum of the spectrum of a LP-FBG can be explained in terms of the quenching and replacement of hydrogen in the core. The amount of hydrogen depleted by quenching in the core turns out to be small, as low as 6%, in LP-FBGs, unlike Malo's result for SP-FBGs, which was as high 80%.

In this paper, after describing the conditions for LP-FBG fabrication, we present experimental observations of the evolution of their transmission spectrum over a period of 500 h at room temperature. We then explain our physical model for the dynamic evolution of the spectrum. Using theoretical calculations of hydrogen diffusion and comparing the experiments
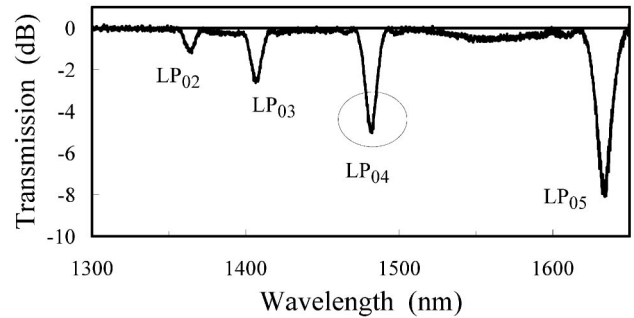

Fig. 1. Transmission spectrum of a LP-FBG. The evolution of the LP_{04} mode is tracked and analyzed in these experiments.

with a fiber Bragg grating's simulation code, we show that the dynamic evolution can be explained entirely by our model. The fraction of the hydrogen that is quenched in the fiber core by UV irradiation is discussed briefly.

2. Experiment

The optical fiber used in these experiments is standard germanium-doped single-mode fiber (SMF-28, Corning). To increase its UV photosensitivity, we loaded hydrogen gas into the fiber at 100 atm at room temperature for 10 days and then stored it in a freezer at -70 °C before use. The resin coating was removed just before exposure to the UV laser light. We fabricated a LP-FBG by exposing the fiber to KrF excimer laser light through multiple slits in thin stainless steel with a 50% opening factor and a 518 μm period. The fiber holder together with the multiple slits was moved across the laser beam in the longitudinal direction of the fiber. The beam size was 15 mm × 15 mm, and the total length of the LP-FBG was 40 mm, with 77 periods, each exposed for 45 s. The laser fluence was 280 (mJ/cm^2)/pulse at the position of the fiber with a 20 Hz repetition rate. A weak tension of 30 g at. wt. was applied to the fiber to keep it stretched.

After exposure of the fiber to the UV laser, we kept the fiber at room temperature and tracked the dynamic evolution of its spectrum for more than 500 h. Figure 1 shows the transmission spectrum for wavelengths of 1300–1700 nm, measured with a white-light source after completion of the experiments described below. In this study we tracked the LP_{04} mode at ~1480 nm after identifying the mode number as described previously,[3] using a wideband strong light source (Thorlabs-ASE-7701-AP).

The LP-FBG had a transmission minimum of -2.2 dB at a wavelength of 1485 nm just after fabrication by exposure to UV laser light, as shown by curve (A) of Fig. 2. The spectrum evolved from (A) to (B) in 160 min, to (C) after 1500 min (25 h), and reached a steady-state spectrum (D) after 30,000 min (500 h). The upswing in the wavelength is large, nearly 80 nm. The initial transmission minimum of -2.2 dB later reached -5 to -6 dB. The wavelength and the transmission minimum are plotted in Figs. 3(a) and 3(b), respectively.
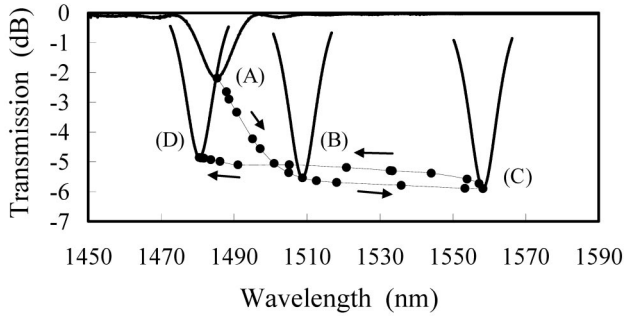
Fig. 2. Dynamic evolution of the transmission spectrum of LP-FBG. The trajectory of its minimum is shown by closed-circle data points.

3. Model for the Evolution of the LP-FBG Spectrum

Our physical model for the dynamic evolution of the LP-FBG is illustrated schematically in Fig. 4. The radial distributions of the molecular-hydrogen concentration are depicted on the left-hand side of the figure for six stages, along with the corresponding radial distributions of the refractive index at the right. The magnitudes in the figure are not to scale but are drawn for ease in understanding of the physical model. The stages in the evolution of the spectrum depicted in Fig. 4 are as follows:

A. Stage 1

Stage 1 is before exposure to UV laser light. Hydrogen molecules are distributed uniformly across the fiber as shown in (H-1) at the left in Fig. 4. The refractive index is raised uniformly both in the core
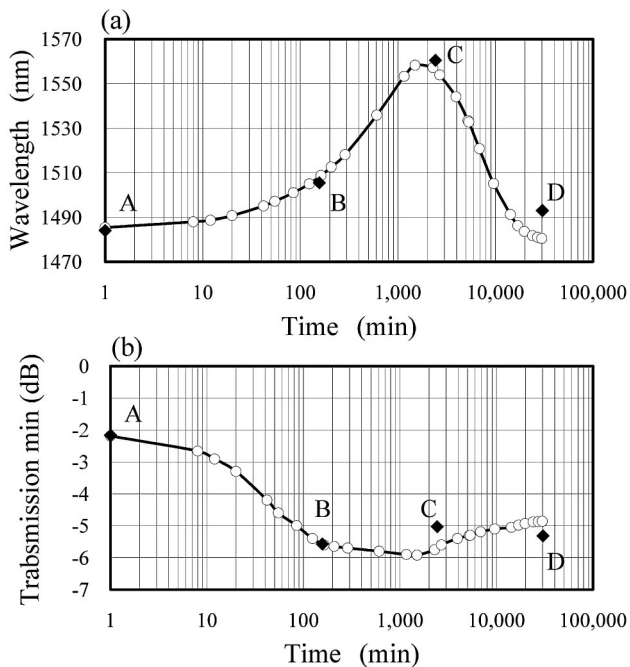

Fig. 3. (a) Wavelength and (b) transmission minimum of the LP-FBG spectrum plotted against time. Filled diamonds A–D correspond to the time slices shown in Fig. 4. Their magnitudes are the results of computer simulation.

and in the cladding by an amount that is due to the loaded hydrogen. The profile shape is the same as that without hydrogen loading.

B. Stage 2

Immediately after exposure of the fiber to UV laser light, which we refer to as time slice A, the refractive index is raised at the core. In this stage, hydrogen molecules are dissociated by the UV laser light. In the fiber core a fraction of the dissociated atoms reacts with dopant germanium to form a Ge—OH bond, while in the fiber cladding they just recombine to form hydrogen. Thus hydrogen is consumed in the fiber core and its concentration decreases there; that is, quenching takes place as shown by (H-2) in Fig. 4. The refractive index increases in the core owing to the photosensitivity of germanium to UV irradiation. At the same time, the index simultaneously decreases by an amount proportional to the amount of hydrogen quenched at the fiber core [indicated by the dotted line (R-2)]. The longitudinal distributions of the hydrogen concentration and the refractive index in the fiber core are shown in Fig. 5.

C. Stage 3

Hydrogen molecules migrate into the depleted fiber core from the surrounding region of the fiber cladding by diffusion. The amplitude of modulated refractive index Δn_{mod} increases until it returns to the level that existed before the quenching of molecular hydrogen by the UV laser light. The time after which hydrogen filling has been completed corresponds to time slice B.

D. Stages 4 and 5

After completion of hydrogen refilling into the core, the hydrogen molecules in the cladding and in the core start to diffuse out of the fiber. We define time slice C as the time of the maximum difference between on-axis hydrogen concentration and that averaged over the cross section, as described in Section 4 below.

E. Stage 6

When the hydrogen molecules have all diffused outward, the refractive index settles down to its value without hydrogen, as depicted by (R-6) in Fig. 4.

Next we examine this model quantitatively with the aid of hydrogen diffusion theory and a simulation code for fiber Bragg gratings.

4. Theory of Hydrogen Diffusion

The diffusion of hydrogen molecules can be described by the diffusion equation

$$\frac{\partial C}{\partial t} - D\nabla^2 C = 0, \qquad (3)$$

where C is the hydrogen concentration and D is the diffusion coefficient. Coefficient D for hydrogen in silica glass is given by Lemaire[4] as
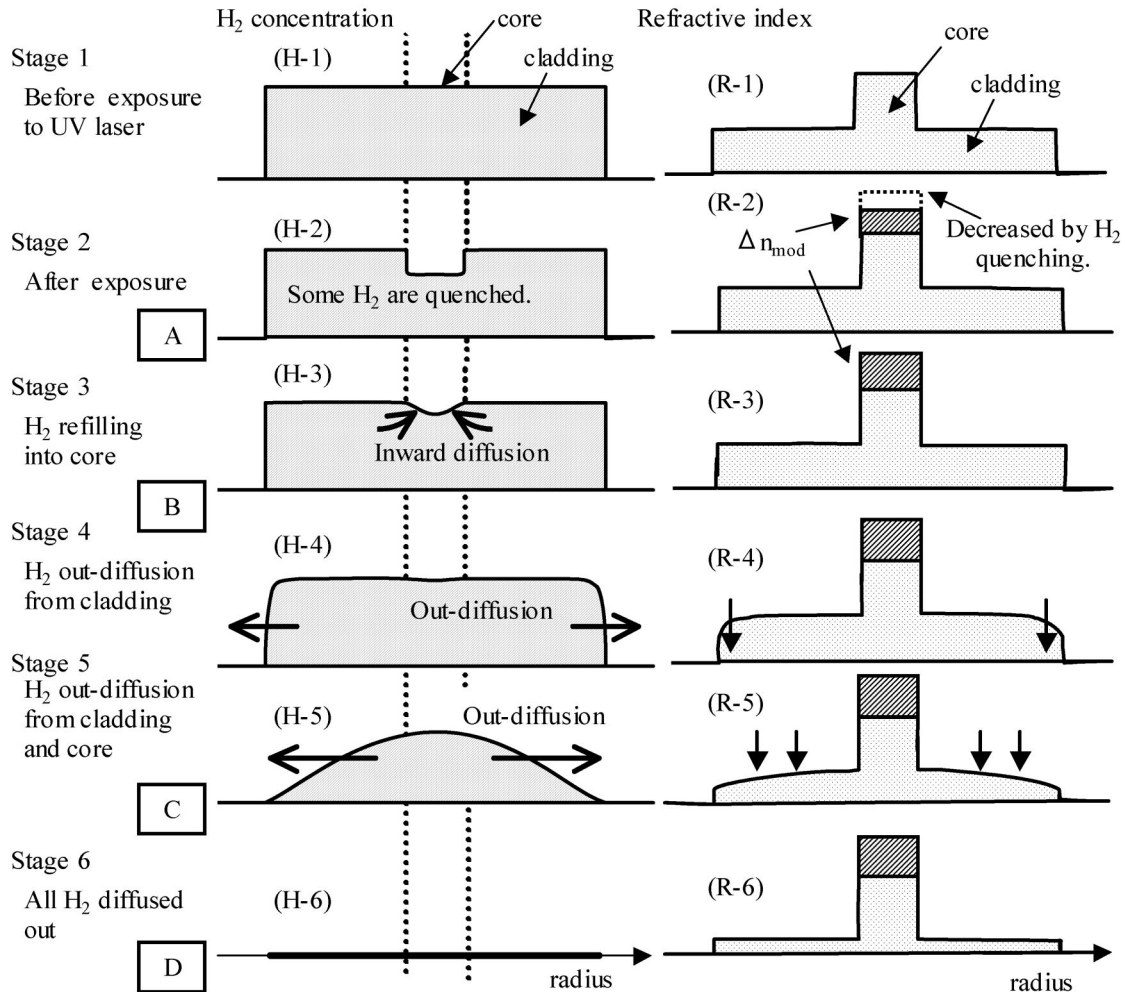
Fig. 4. Model for the evolution of the spectrum. The radial profiles of the hydrogen concentration (left) and the refractive index (right) are shown for six stages. A–D correspond to time slices discussed in the text.

$$D \left[\text{cm}^2\right]/s = 2.83 \times 10^{-4} \exp\left(-\frac{40.19 \left[\text{kJ/mol}\right]}{RT}\right),$$

$$\tag{4}$$

where $R = 8.31$ (J/K) mol is the gas constant and T is given in degrees kelvin. A rigorous solution in cylindrical coordinates is given by Crank.[5] For boundary conditions of

$$\begin{aligned} C = C_1, & \quad r = a, \quad t \geq 0, \\ C = C_0, & \quad r < a, \quad t = 0, \end{aligned} \tag{5}$$

the solution is

$$\frac{C - C_0}{C_1 - C_0} = 1 - \frac{2}{a} \sum_{n=1}^{\infty} \frac{J_0(r\alpha_n)}{\alpha_n J_1(a\alpha_n)} \exp\left(-D\alpha_n^2 t\right), \tag{6}$$

where α_n is determined from the zero point of the Bessel function, $J_0(\alpha_n a) = 0$. For $C_1 = 0$ and $C_0 = 1$ we get the solution for outward diffusion from a profile with an initial uniform distribution. For $C_1 = 1$ and

$C_0 = 0$ we obtain the solution for inward diffusion. Calculated profiles for the radial distribution are shown for several values of Dt/a^2 in Figs. 6(a) and 6(b) for outdiffusion and indiffusion, respectively. The amount of hydrogen that diffuses out from the fiber, $M(t)$, can be obtained by integration of the concentration with respect to time and is given by

$$\frac{M(t)}{M(\infty)} = 1 - \sum_{n=1}^{\infty} \frac{4}{a^2 \alpha_n^2} \exp\left(-D\alpha_n^2 t\right), \tag{7}$$

where $M(\infty)$ is the total amount that diffuses out.

The time to refill the depleted core after quenching (stage 3) can be estimated as the inward diffusion time $t_{\text{refill}} \sim a_{\text{core}}^2/D$. For a core radius $a_{\text{core}} = 4.5 \ \mu\text{m}$, t_{refill} becomes 157 min. Similarly, for a cladding radius $a_{\text{clad}} = 62.5 \ \mu\text{m}$, the time to complete the outward diffusion, that is, to finish stage #6, is $t_{\text{outdiff}} = a_{\text{clad}}^2/D \sim 30,300$ min. Here diffusion coefficient D is $2.15 \times 10^{-15} \ \text{m}^2/\text{s}$ according to Eq. (4) for 22 °C. Refilling time $t_{\text{refill}} = 157$ min corresponds to time slice B, and the time for outward diffusion,
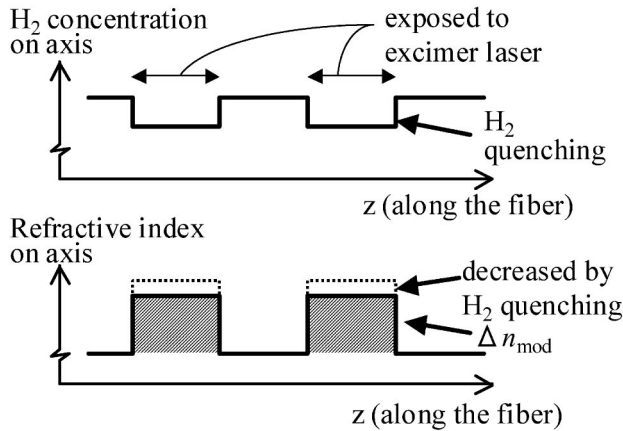
Fig. 5. Hydrogen concentration and refractive index along the axis of the fiber in our model.

Fig. 7. Hydrogen concentrations during diffusion: $C_{\text{on-axis}}$ is the on-axis value, C_{average} is the value averaged over the fiber's cross section, and $C_{\text{difference}}$ is the difference between the two.

$t_{\text{outdiff}} = 30,300$ min, corresponds to time slice D in our model of Fig. 4.

The transmission minimum becomes deeper as the amplitude of the refractive-index modulation increases from that of (R-2) in Fig. 4 to that of (R-3) during refilling of the core until to time B. Thus, the transmission minimum started at -2.2 dB (time slice A), deepened to -5 to -6 dB at time slice B, and remained nearly the same thereafter, as shown in Fig. 3(b).

When hydrogen molecules diffuse out of the fiber in stages #4 and #5, the concentration decreases first at the outside of the fiber cladding and then in the core. The evolution of the radial profile of the hydrogen concentration can be analyzed by use of Eqs. (6) and (7). The result is shown in Fig. 7, which shows the average concentration C_{average} calculated from Eq. (7)
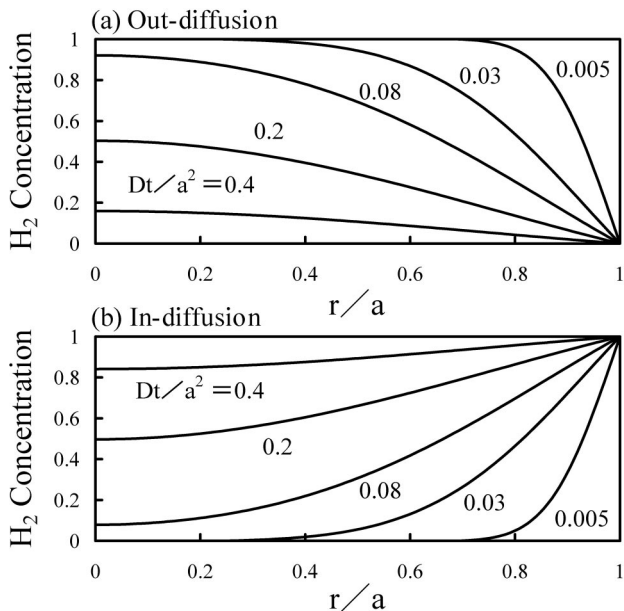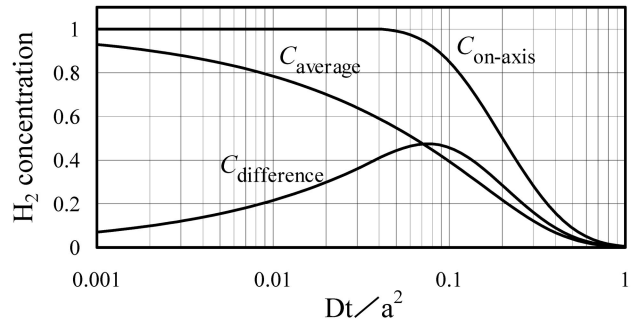
and the on-axis concentration according to Eq. (6). $C_{\text{difference}}$, the difference between the two, reaches a maximum at the time when $Dt/a_{\text{clad}}^2 = 0.08$ and decreases thereafter. The wavelength of the LP-FBG is given by Eq. (1). n_{eff}^{01} follows closely the refractive index of the fiber core, and n_{eff}^{0m} follows the average of the refractive index over the cross section. Therefore the effect of hydrogen on the wavelength should yield a wavelength evolution similar to that of the time dependence of $C_{\text{difference}}$ shown in Fig. 7. The time that corresponds to $Dt/a_{\text{clad}}^2 = 0.08$ gives $t_{\text{peak}} = 2430$ min. After this t_{peak} (time slice C), the wavelength should decrease.

The results of this analysis of the temporal behavior are shown in Figs. 3(a) and 3(b). There the filled diamonds show the calculations for times A–D, which agree well with the experimental times (Fig. 8). In Section 5 we analyze the magnitudes of the wavelength shifts and changes in the transmission minimum, using a computer simulation code.

5. Simulation

We used the IFO_grating code from the Optiwave Corporation.[6] This code calculates the transmission and reflection spectra for specified fiber conditions, i.e., the refractive-index distributions in the fiber core and cladding and the Bragg grating conditions, i.e., grating period Λ, modulated refractive index in the core Δn_{mod}, and grating length L. The fiber conditions are defined by the specifications of SMF-28 single-mode fiber. The specific difference of the refractive

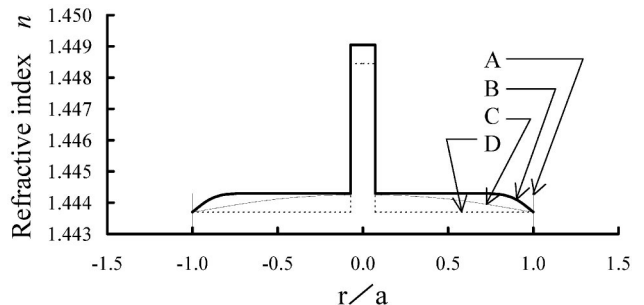Fig. 6. Radial profiles of hydrogen concentration during outward diffusion and inward diffusion.

Fig. 8. Radial profiles of the refractive index. A–D correspond to the time slices in Table 1 and Fig. 4.

Table 1. Refractive Indices for Four Time Slices, A–D

Time Slice	Stage (Time)	Condition	Refractive Index		
			n_{core}, $0 < r < 4.5$ μm	$n_{cladding}$, $4.5 < r < 62.5$ μm	$\Delta n_{modulation}$
A	stage 2 ($t = 0$ min)		1.449,050	1.444,300	0.000,075
B	end of stage 3 ($t = 157$ min)	$Dt/a_{core}^2 = 1$	1.449,050	1.444,300–1.443,700	0.000,111
C	stage 5 ($t = 2430$ min)	$Dt/a_{clad}^2 = 0.08$	1.449,000	1.444,250–1.443,700	0.000,111
D	stage 6 ($t = 30,300$ min)	$Dt/a_{clad}^2 = 1$	1.448,450	1.443,700	0.000,111
		Difference between A and D	$n_{core}^{A-D} = 0.000\,600$	$n_{cladding}^{A-D} = 0.000\,600$	$\Delta n_{core}^{A-D} = 0.000\,036$

index is $\Delta = (n_{core} - n_{clad})/n_{core} = 0.36\%$, with $n_{clad} = 1.4437$ at 1550 nm. The core and cladding diameters are $2a_{core} = 9$ μm and $2a_{clad} = 125$ μm, respectively. Outside the fiber, air cladding with $n = 1$ is assumed. Rectangular modulation of the grating was assumed, and we adjusted its amplitude by fitting to experiment. The grating's period is $\Lambda = 518$ μm, and its total length is $L = 40$ mm.

The refractive indices n_{core} and n_{clad} just after the fabrication (time slice A) were determined by fitting of the computed wavelength to that of experiments. We determined Δn_{mod} by fitting the transmission minimum to experimentally observed values. These values are listed in Table 1 for time slice A, and the spectrum is shown in Fig. 9.

Two parameters must be clarified here. One is n_{H_2}, the refractive index caused by hydrogen. The other is $\delta n_{H_2-quench}$ the fraction of n_{H_2}, lost by quenching during exposure to the UV laser light. The radial distribution of hydrogen can be obtained from Fig. 6. At time A, the refractive indices n_{core} and n_{clad} include n_{H_2}, and Δn_{mod} is reduced by the quenched fraction $\delta n_{H_2-quench}$. By increasing Δn_{mod} from the value for time A, i.e., 0.075×10^{-3}, we adjusted the transmission minimum to fit the experimental value at time B, which yields $\Delta n_{mod} = 0.111 \times 10^{-3}$. This value should remain constant thereafter in our model. The increase in Δn_{mod} from A to B raised the wavelength by ~20 nm. The contribution to the refractive index owing to outdiffusion of hydrogen is given by

$$n_{clad}(r, t) = n_{clad}^D + n_{H_2}(r, t)$$

$$= n_{clad}^A + n_{H_2}[C(r, t) - C_0]/C_0, \quad (8)$$

where n_{clad}^D is the cladding index without hydrogen, i.e., at time D. Using the radial distribution of the hydrogen concentration $C(r, t)/C_0$ and adjusting its magnitude by varying n_{H_2} to fit the wavelength at times C and D consistently, we obtain

$$n_{H_2} = 0.600 \times 10^{-3}. \quad (9)$$

In this calculation, Δn_{mod} is the value for time B, i.e., 0.111×10^{-3}. This value of n_{H_2} agrees well with our previous result (6.70×10^{-4}).[3] It should be noted that the change in the refractive index caused by the hydrogen loading, n_{H_2}, is large, approximately 5–6 times greater than Δn_{mod} induced by UV irradiation. These results are summarized in Table 1. The differences in n_{core} and n_{clad} between times A and D both correspond to n_{H_2}. The increase in Δn_{mod} from time slice A to B corresponds to the amount of quenching by the UV irradiation, that is,

$$\delta n_{H_2-quench} = 0.036 \times 10^{-3} \cong 6\% \times n_{H_2}. \quad (10)$$

6. Discussion

The evolution of LP-FBGs after fabrication by exposure to UV lasers after hydrogen loading is characterized by two distinct features: a large wavelength upswing and a deepening of the transmission minimum as if the modulation of the grating had gotten stronger. Bakhti *et al.* have proved that the former is due to outdiffusion of the hydrogen that was loaded into the fiber to enhance its UV photosensitivity. But, to the best of our knowledge, the behavior of the transmission minimum was not explained before. Using the theory of Malo *et al.*,[2] according to which the hydrogen in the fiber core gets quenched by UV irradiation and is subsequently refilled by inward
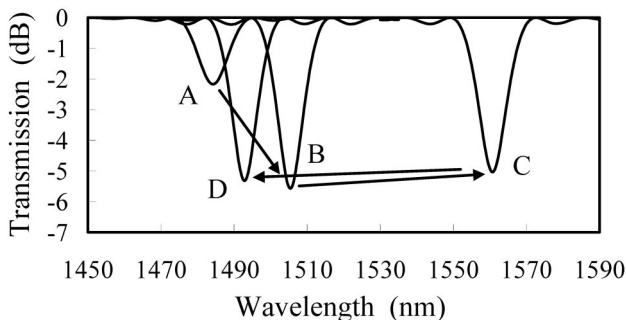

Fig. 9. Transmission spectra obtained by computer simulation.

diffusion from surrounding cladding, we have demonstrated that the increase in Δn_{mod} attributable to hydrogen refilling causes the transmission minimum to decrease.

The amount of the refractive index of hydrogen molecules has turned out to be $n_{H_2} = 0.600 \times 10^{-3}$ in our analysis as described in Eq. (9). This is the index increased by the dissolved hydrogen saturated by its loading at 100 atm. In Malo's experiment[2] the index increase is 0.05% of the effective refractive index of the optical fiber used, which becomes $1.444 \times 0.05\%$, or 0.7×10^{-3} with 100 atm loading (1 mol. % saturation) and with SMF28 optical fiber. The agreement of our index increase with Malo's is quite remarkable.

The fraction of hydrogen molecules quenched by UV irradiation is roughly 6% relation [Eq. (10)] of the hydrogen load. Malo's experiment for SP-FBGs yielded a fraction much larger than ours, i.e., approximately 70–80%, as shown in Fig. 1(a) of Ref. 2. The difference is likely caused by the magnitude of their energy of UV irradiation, which appears to be much larger than ours. Because the index change owing to the loaded hydrogen, i.e., n_{H_2} in our analysis, is approximately 5–6 times greater than Δn_{mod} induced by the UV irradiation, if approximately 70–80% of hydrogen were quenched, Δn_{mod} could easily become negative, which would means that the grating phase could be inverted in the longitudinal direction of the fiber. If this occurred, the transmission minimum should go to zero first and grow later. Of course, no such evolution has been observed.

The value of 6% for the quenching must be closely related to the efficiency of the photoinduced refractive-index increase. Theoretical analysis evaluating this parameter quantitatively is needed for an understanding of the efficiency of UV irradiation.

7. Conclusions

The transmission spectra of LP-FBGs fabricated by exposure of hydrogen-loaded fiber to UV laser light manifest a large-scale evolution in both their wavelength and their transmission minima during approximately two weeks at room temperature. The wavelength experiences a large upswing, and the transmission minimum deepens as if the grating strength had increased. Bakhti et al.[1] have shown that the evolution of the wavelength is caused by outdiffusion of hydrogen from the fiber, but the evolution of the transmission minimum was not explained. Using the theory of Malo et al.[2] for quenching and refilling of hydrogen in SP-FBGs, we have explained the dynamic evolution of the transmission minimum for LP-FBGs. That is, just after exposure to the UV laser, the modulation of refractive index Δn_{mod} is reduced by an amount induced by hydrogen quenching in the fiber core owing to UV irradiation. Subsequently the hydrogen is replaced by inward diffusion of hydrogen from the surrounding cladding. This refilling effectively increases Δn_{mod} enough to recover the previous value without hydrogen. This causes a substantial deepening of the transmission minimum. We have found that the amount of hydrogen quenched by the UV irradiation is 6% of the hydrogen load.

References

1. F. Bakhti, J. Larrey, P. Sansonetti, and B. Poumellec, "Impact of hydrogen in-fiber and out-fiber diffusion on central wavelength of UV-written long period gratings," in *Bragg Gratings, Photosensitivity and Poling in Glass Fibers and Waveguides: Fundamentals and Applications,* Vol. 17 of OSA Technical Series (Optical Society of America, 1997), pp. 55–57, paper BsuD4-1.
2. B. Malo, J. Albert, K. O. Hill, F. Bilodeau, and D. C. Johnson, "Effective index drift from molecular hydrogen diffusion in hydrogen-loaded optical fibres and its effect on Bragg grating fabrication," Electron. Lett. **30,** 442–444 (1994).
3. Y. Masuda, M. Nakamura, C. Komatsu, K. Fujita, M. Yamauchi, M. Kimura, Y. Mizutani, S. Kimura, Y. Suzaki, T. Yokouchi, K. Nakagawa, and S. Ejima, "Wavelength evolution of fiber Bragg gratings fabricated from hydrogen loaded optical fiber during annealing," J. Lightwave Technol. **22,** 934–941 (2004).
4. P. J. Lemaire, "Reliability of optical fibers exposed to hydrogen: prediction of long-term loss increases," Opt. Eng. **30,** 780–789 (1991).
5. J. Crank, *The Mathematics of Diffusion* (Clarendon, 1975), p. 73.
6. "IFO_Grating," integrated and fiber optical gratings design software program (Optiwave Corporation, Ottawa, 2001).